# Self-Assembled Tat Nanofibers as Effective Drug Carrier and Transporter

*Pengcheng Zhang, Andrew G. Cheetham, Yi-An Lin,Honggang Cui*[*]

Department of Chemical and Biomolecular Engineering, and Institute for NanoBioTechnology, The Johns Hopkins University, Baltimore, MD 21218, United States

[*]Email: hcui6@jhu.edu

**CONTENTS**

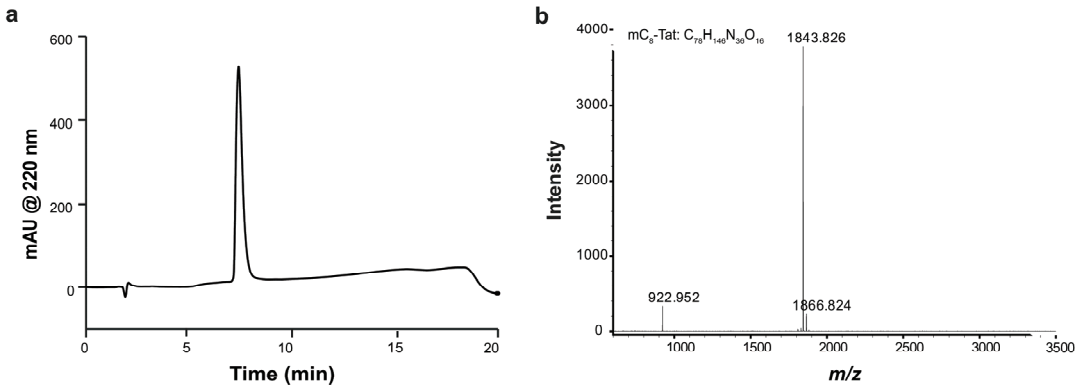


**Figure S1.** RP-HPLC (a) and MALDI-TOF MS (b) characterization of $mC_8$-Tat. The RP-HPLC spectrum confirms the purity of the product (>99%). The peaks at 922.952, 1843.826, and 1866.824 correspond to $[M+2H]^{2+}$, $[M+H]^{+}$ and $[M+Na]^{+}$, respectively.

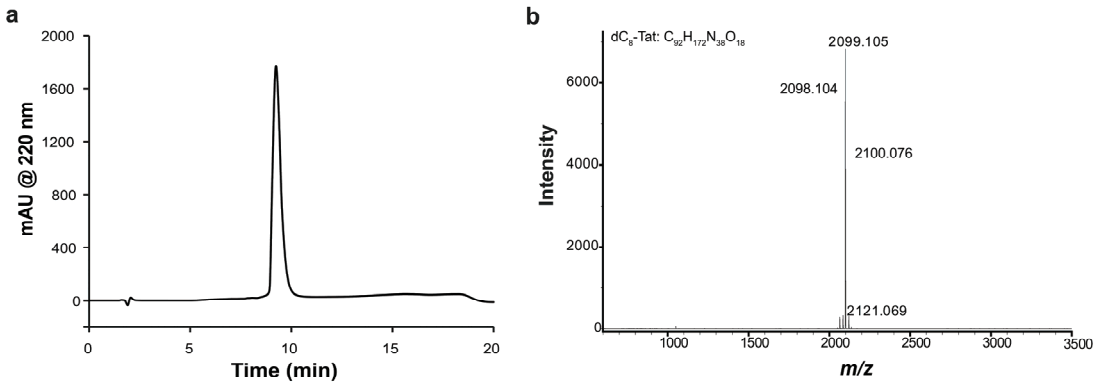


**Figure S2.** RP-HPLC (a) and MALDI-TOF MS (b) characterization of $dC_8$-Tat.The RP-HPLC spectrum confirms the purity of the product (>99%). The peaks at 2099.105 and 2121.069 correspond to $[M+H]^+$ and $[M+Na]^+$, and other peaks are the isotopic peak of $[M+H]^+$.

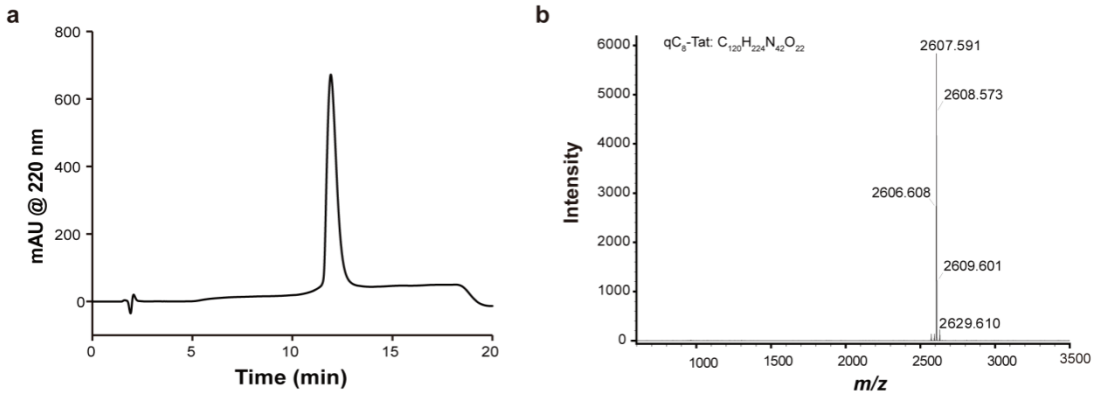


**Figure S3.** RP-HPLC (a) and MALDI-TOF MS (b) characterization of $qC_8$-Tat.The RP-HPLC spectrum confirms the purity of the product (>99%). The peaks at 2607.591 and 2629.610 correspond to $[M+H]^+$ and $[M+Na]^+$, and other peaks are the isotopic peak of $[M+H]^+$.

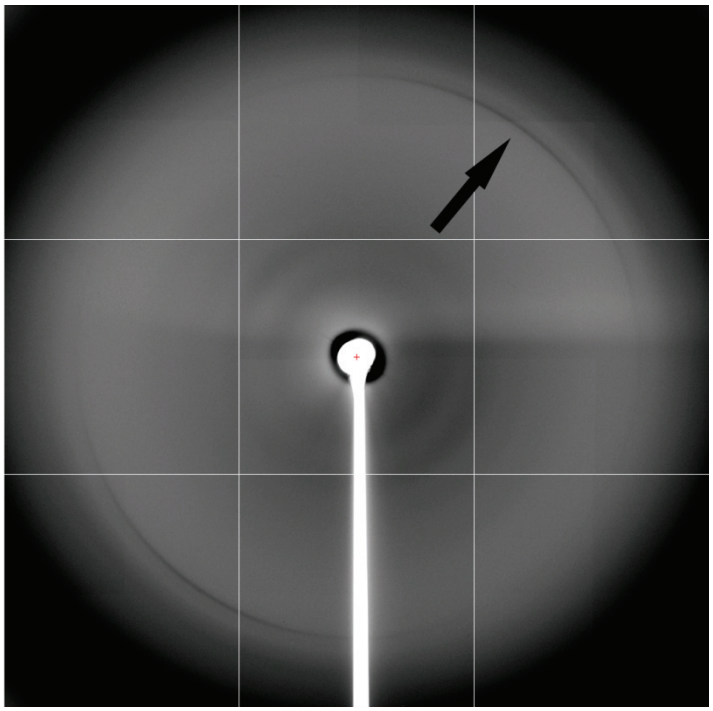

**Figure S4.** Wide angle X-ray scattering 2-D pattern collected from an aqueous solution of Tat nanofibers. The reflection (marked with black arrow) corresponds to a *d*-spacing of 4.7 Å, a signature for *β*-sheet assemblies. The observation of two arcs instead of a Debye-Scherrer ring is due to the alignment of Tat nanofiber by pipetting during the sample preparation.

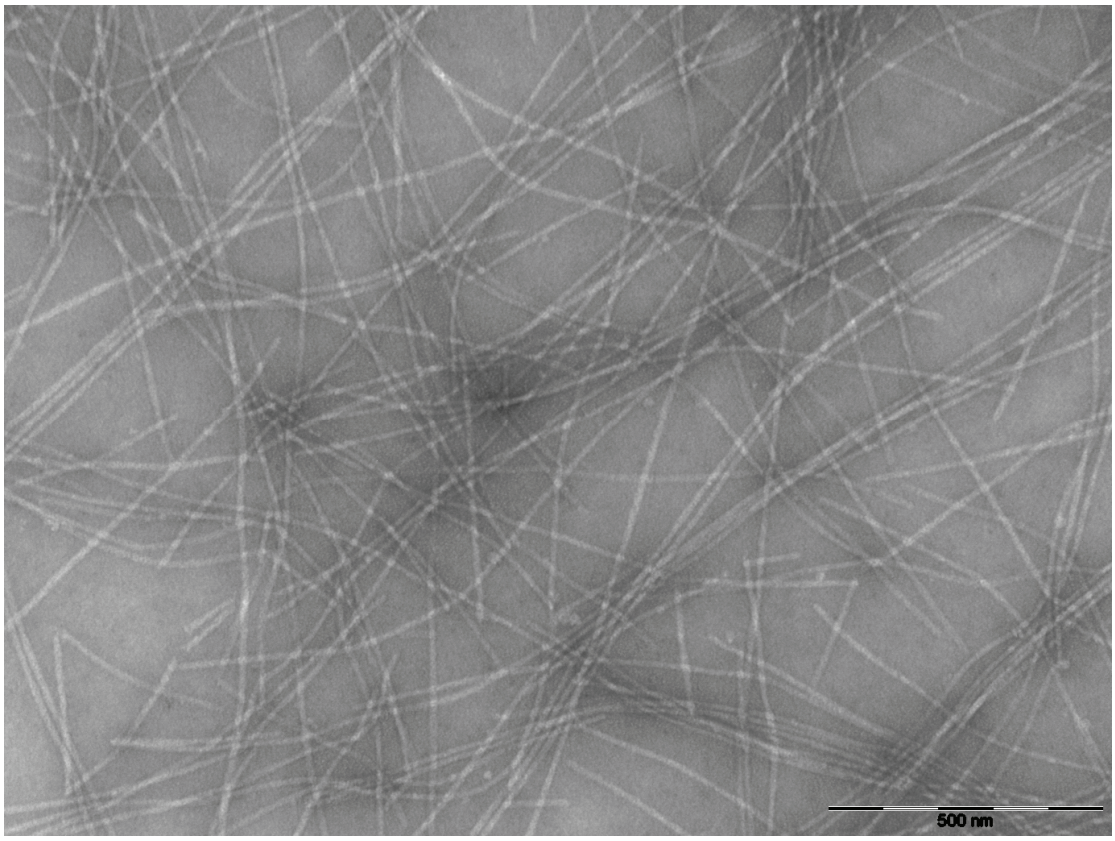


**Figure S5.** TEM image of nanofibers formed by $qC_8$-Tat in DPBS at 2 mM. Uranyl acetate (2 wt%) was used as a negative staining agent

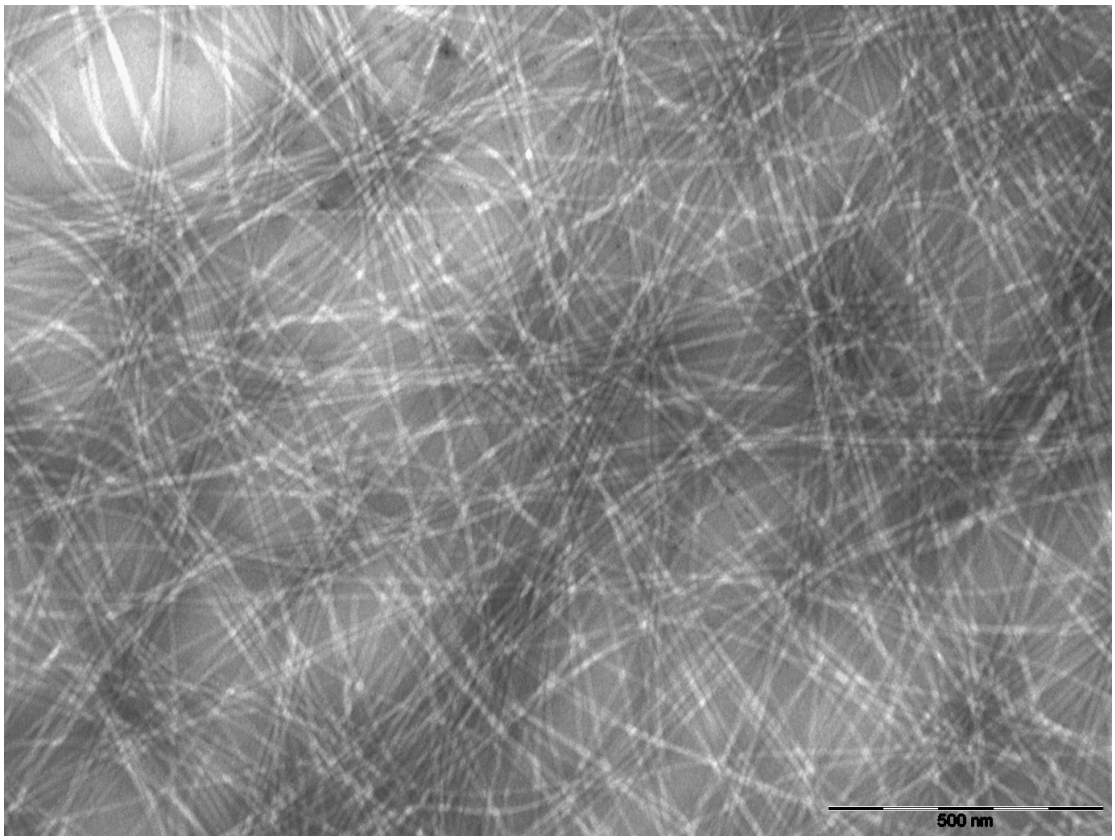


**Figure S6.** TEM image of nanofibers formed by mixing $qC_8$-Tat (2 mM) with PTX at a molar ratio of 100:1 in DPBS. Uranyl acetate (2 wt%) was used as a negative staining agent

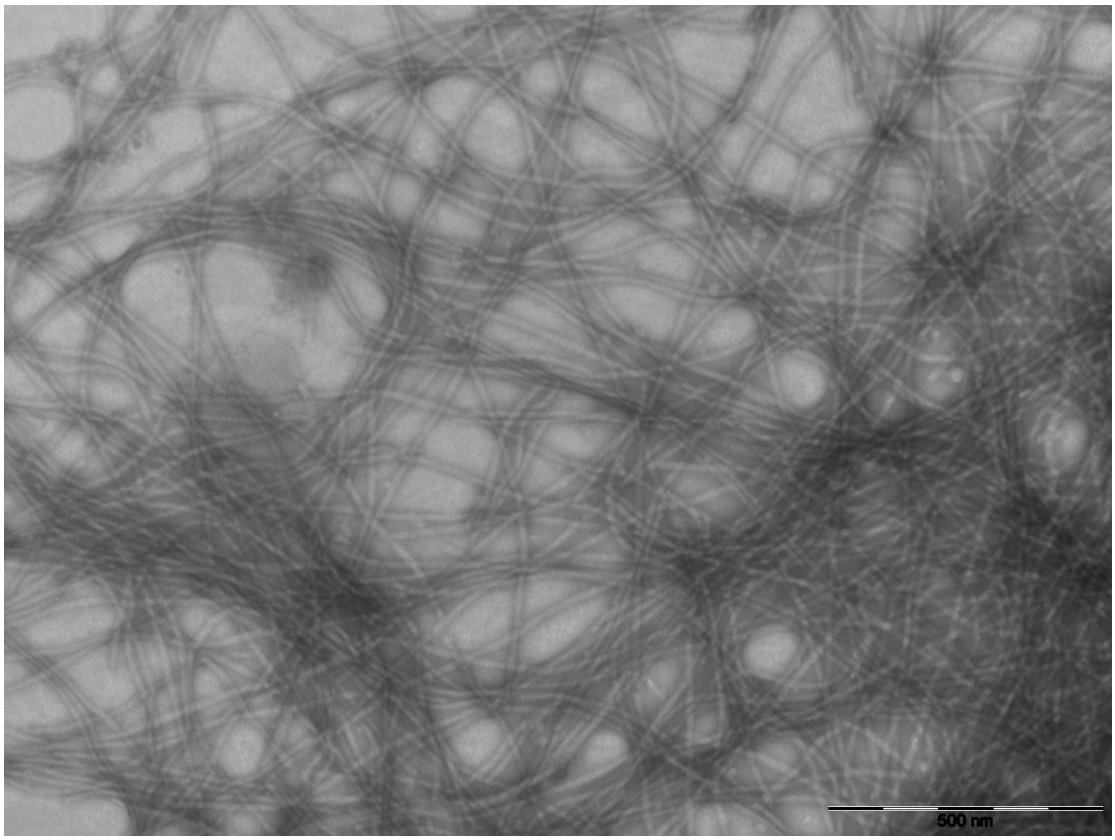


**Figure S7.** TEM image of nanofibers formed by mixing $qC_8$-Tat (2 mM) with PTX at a molar ratio of 20:1 in DPBS. Uranyl acetate (2wt%) was used as a negative staining agent.

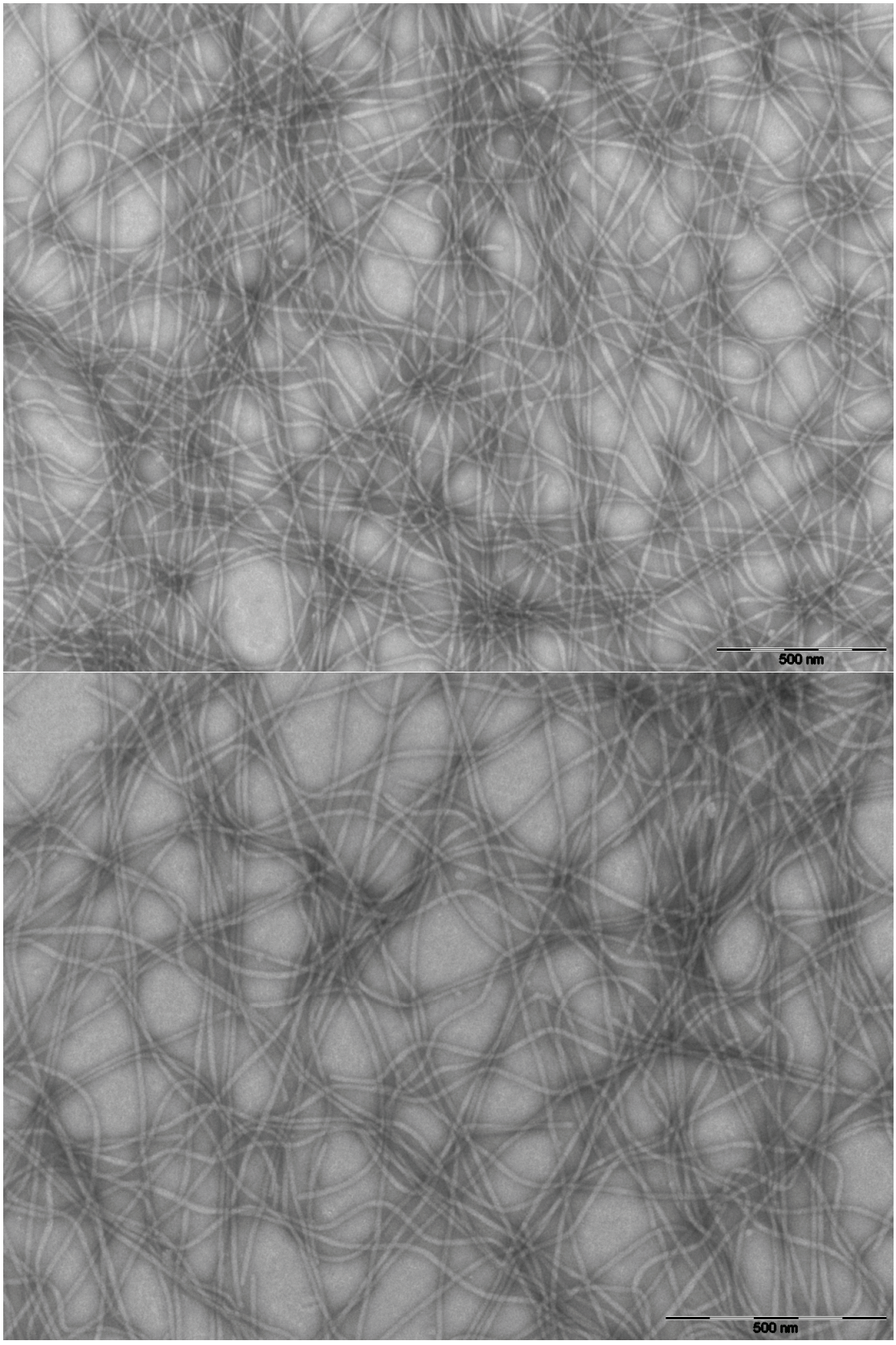


**Figure S8.** TEM image of nanofibers formed by mixing of $qC_8$-Tat (2 mM) with PTX at a molar ratio of 10:1 in DPBS. Uranyl acetate (2 wt%) was used as a negative staining agent.

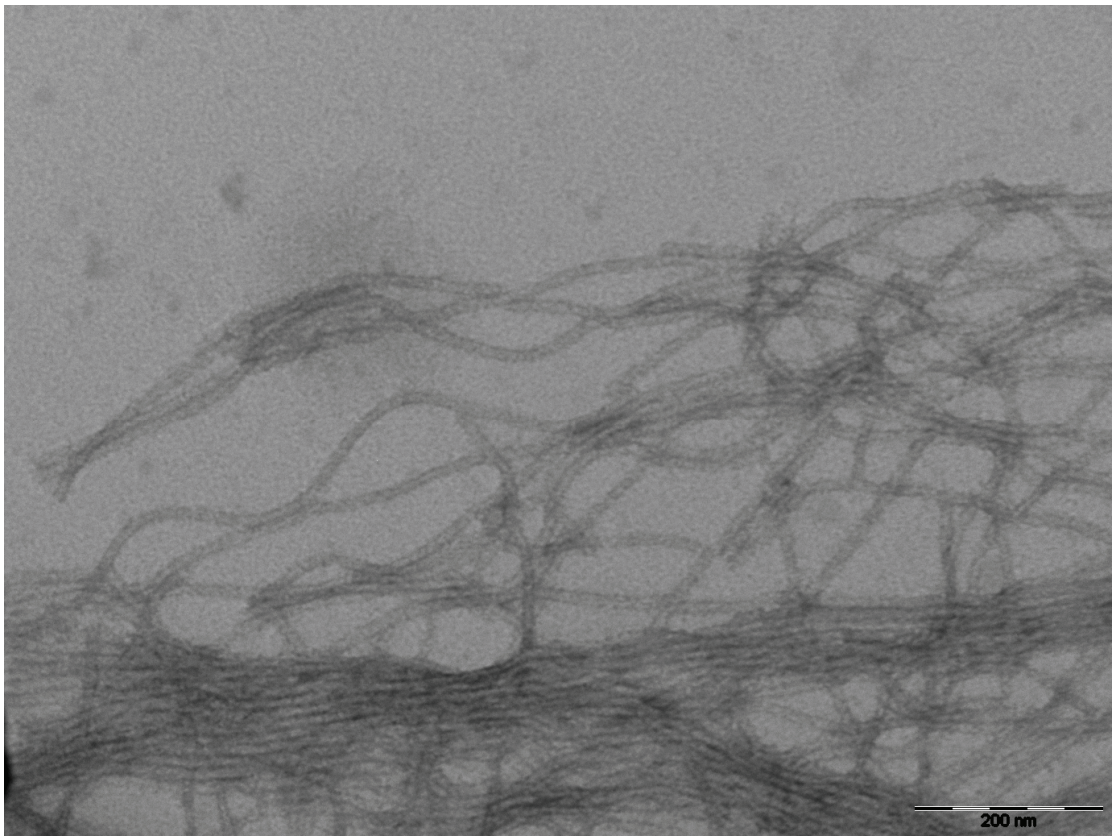


**Figure S9.** TEM image of nanofibers formed by mixing $qC_8$-Tat (2 mM) with PTX at a molar ratio of 20:3 in DPBS. Uranyl acetate (2 wt%) was used as a negative staining agent.

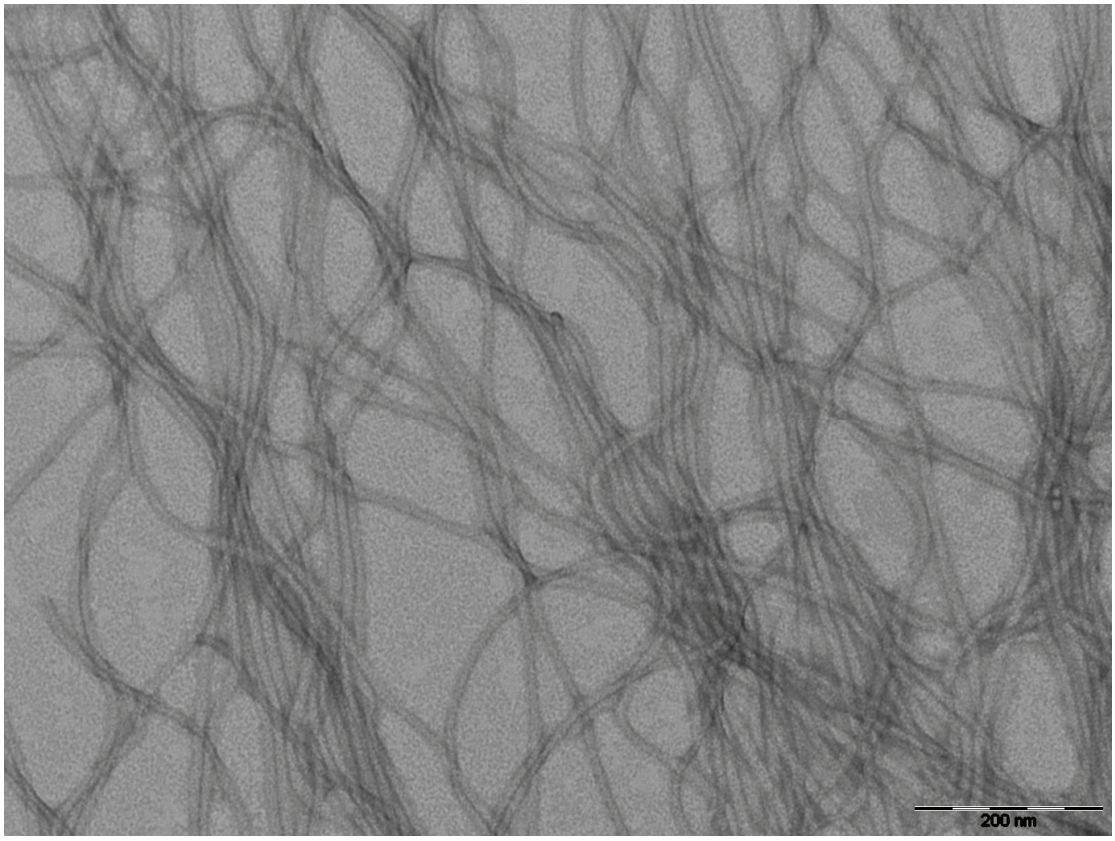


**Figure S10.** TEM image of nanofibers formed by mixting $qC_8$-Tat (2 mM) with PTX at a molar ratio of 5:1 in DPBS. Uranyl acetate (2 wt%) was used as a negative staining agent.

**Table S1.** The diameters of PTX-N with different drug loading. Data were presented as mean ± s.d. (n = 30).

| Conjugate to PTX ratio, (mol/mol) | No drug | 100:1 | 20:1 | 10:1 | 20:3 | 5:1 |
|---|---|---|---|---|---|---|
| Diameter (nm) | 15.0 ± 0.9 | 14.9 ± 0.9 | 14.9 ± 0.8 | 15.0 ± 0.7 | 15.0± 0.8 | 14.8 ± 0.7 |

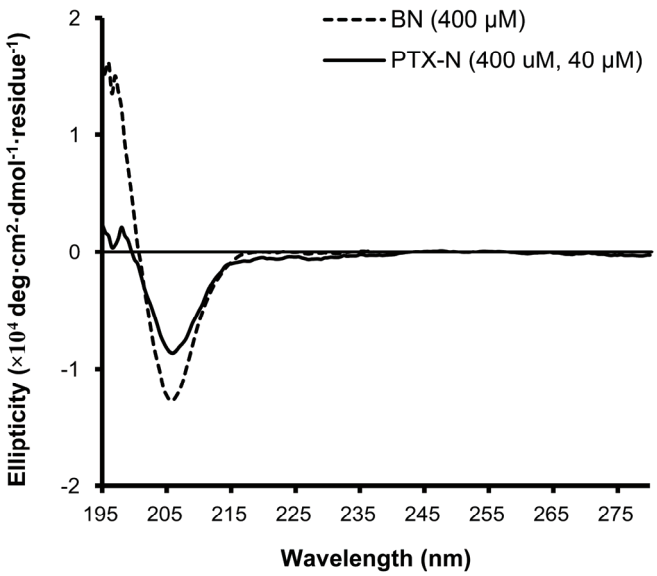


**Figure S11.** Normalized CD spectra of 400 μM blank Tat nanofibers (BN) and Tat nanofibers loaded with PTX (PTX-N, 10:1, mol/mol) in DPBS. Both the blank nanofiber and PTX-N showed signal at around 205 nm indicating a polyproline type II (PPII) like conformation. This experiment suggests that Tat peptides are not accountable for the observed change in nanofiber morphology

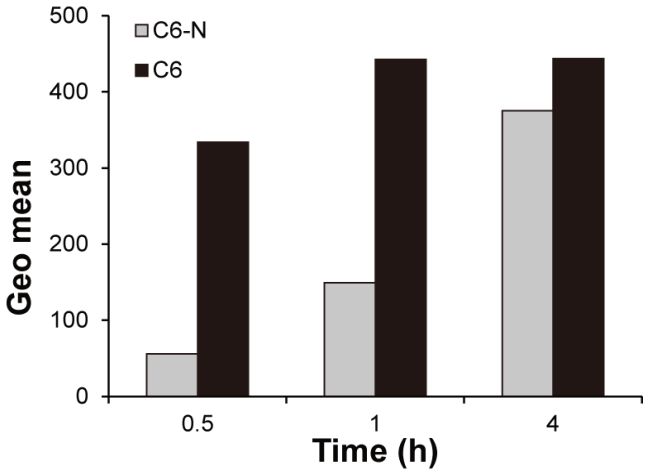


**Figure S12.** Time-course intracellular accumulation of coumrain-6 in KB-3-1 cells after incubation with either 300 nM free coumarin-6 (C6) or coumarin-6 loaded nanofibers (C6-N) for 0.5, 1 and 4 h, as determined by flow cytometry. While the intracellular accumulation kinetics between C6 and C6-N is different, comparable accumulation was achieved after 4 h incubation.

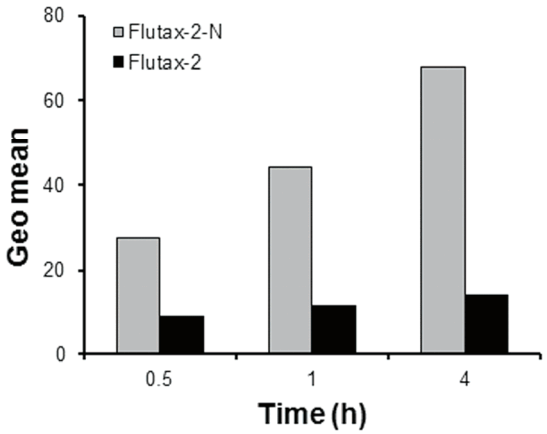


**Figure S13.** Time-course intracellular accumulation of Flutax-2 in KB-3-1 cells after incubation with either 500 nM free Flutax-2 or Flutax-2 loaded nanofibers (Flutax-2-N) for 0.5, 1 and 4 h, as determined by flow cytometry. The intracellular accumulation of Flutax-2-N is more efficient than free Flutax-2.

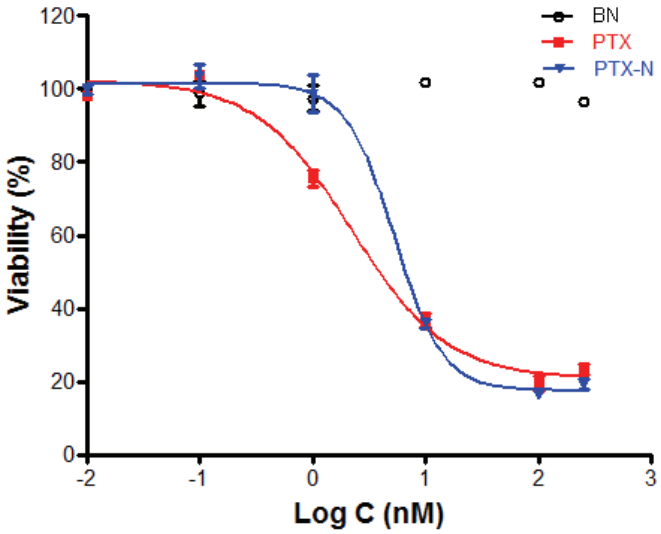


**Figure S14.** Cell viability of A549 non-small cell lung cancer cells treated for 48 h with PTX (0.01 – 250 nM), PTX-N (0.01 – 250 nM PTX and 0.1 – 2500 nM $qC_8$-Tat), or $qC_8$-Tat (0.1 – 2500 nM $qC_8$-Tat). Comparable cytotoxicity was observed for free PTX and PTX-N, indicating encapsulation did not reduce the antitumor activity of paclitaxel to A549. $qC_8$-Tat did not contribute to the cytotoxicity significantly at the concentrations used for paclitaxel encapsulation.

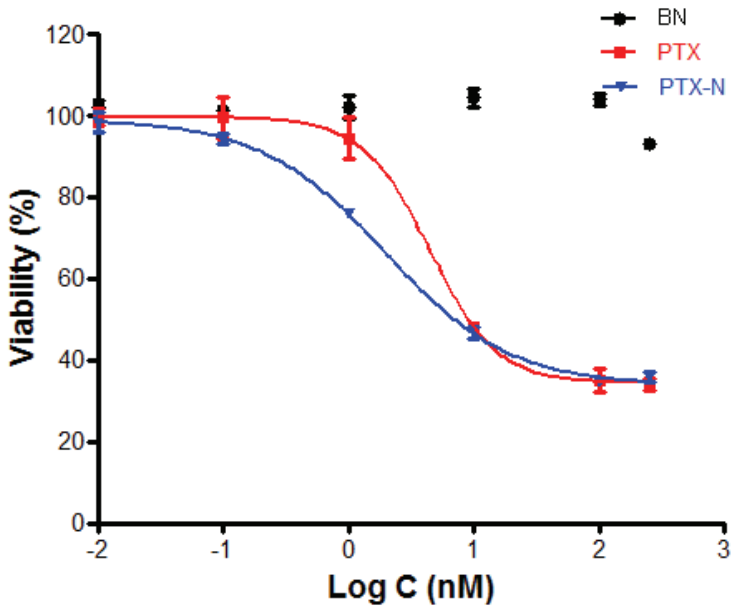


**Figure S15.** Cell viability of MDA-MB-231 breast cancer cells treated for 48 h with PTX (0.01 – 250 nM), PTX-N (0.01 – 250 nM PTX and 0.1 – 2500 nM $qC_8$-Tat), or $qC_8$-Tat (0.1 – 2500 nM $qC_8$-Tat). Comparable cytotoxicity was observed for free PTX and PTX-N, indicating encapsulation did not reduce the antitumor activity of paclitaxel to MDA-MB-231. $qC_8$-Tat did not contribute to the cytotoxicity significantly at the concentrations used for paclitaxel encapsulation.

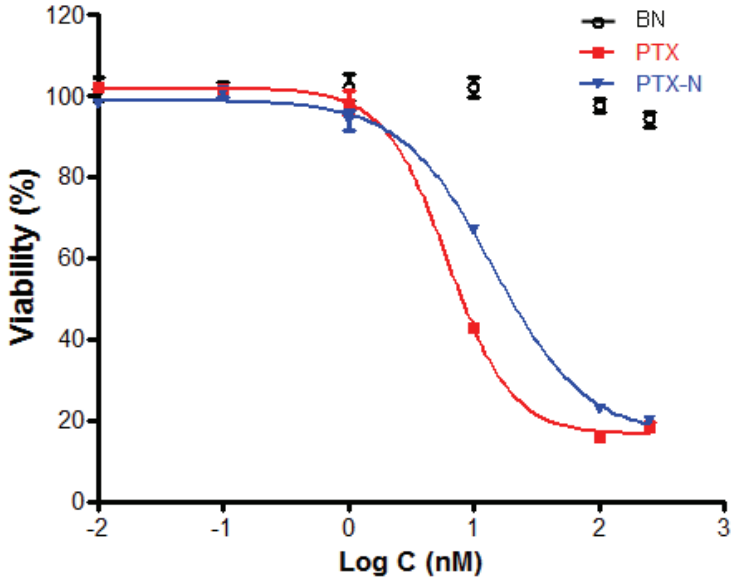


**Figure S16.** Cell viability of OVCAR-8 ovarian cancer cells treated for 48 h with PTX (0.01 – 250 nM), PTX-N (0.01 – 250 nM PTX and 0.1 – 2500 nM $qC_8$-Tat), or $qC_8$-Tat (0.1 – 2500 nM $qC_8$-Tat). Comparable cytotoxicity was observed for free PTX and PTX-N, indicating encapsulation did not reduce the antitumor activity of paclitaxel. $qC_8$-Tat did not contribute to the cytotoxicity significantly at the concentrations used for paclitaxel encapsulation.

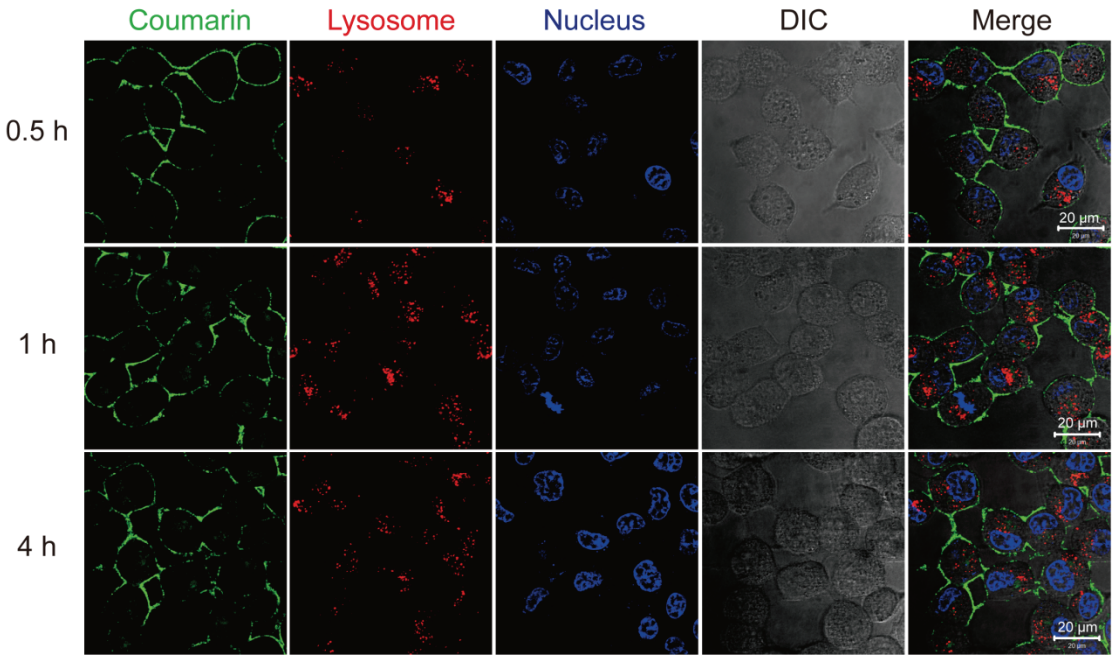


**Figure S17.** Subcellular colocalization of free coumarin-6 (green) in live KB-3-1 with lysosome (Lysotracker red, red) and nucleus (Hoechst 33342, blue) after incubation of cells with 0.3 μM of coumarin-6 for 0.5, 1, and 4 h at 37 $^{o}$C. This experiment reveals clearly coumarin-6 dominantly accumulated in the cell membrane even after 4 h incubation, in sharp contrast to courmarin-6 delivered by Tat nanofibers which accumulated largely within the cells.

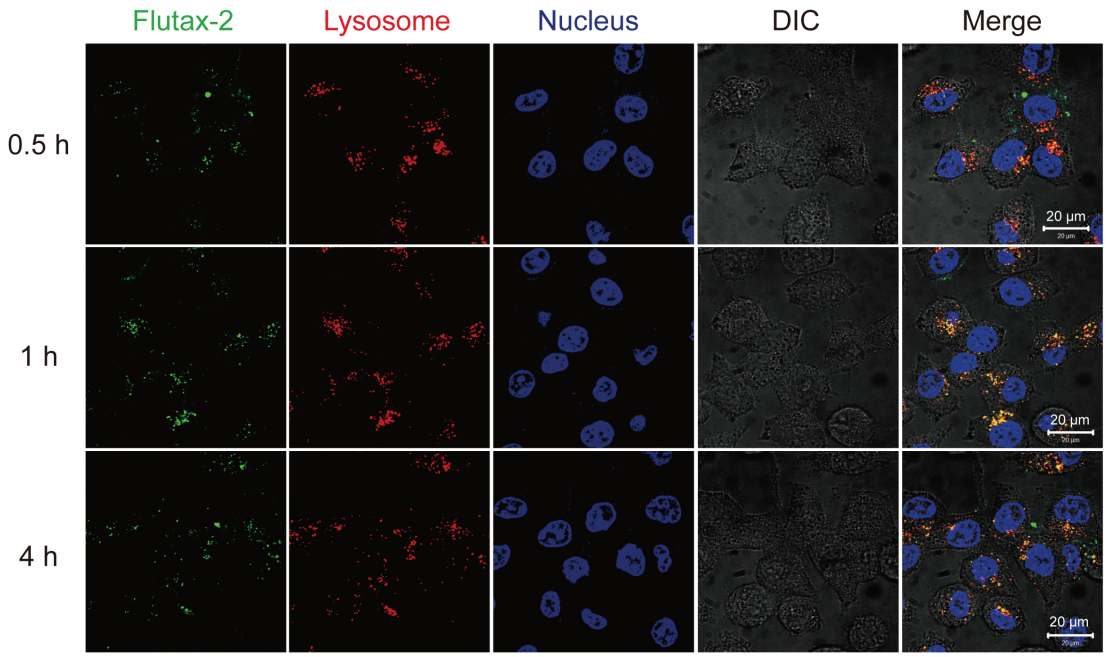


**Figure S18.** Subcellular colocalization of free Flutax-2 (green) in live KB-3-1 with lysosome (Lysotracker red, red) and nucleus (Hoechst 33342, blue) after incubation of cells with 0.5 μM of Flutax-2 for 0.5, 1, and 4 h at 37 $^{o}$C. This experiment reveals lower intracellular accumulation of free Flutax-2 compared with Flutax-2-N. The co-localization of Flutax-2 (green) with lysosome (red) indicates that free Flutax-2 did not enter the cells through free diffusion.